The Preliminary Report on a Three Dimensional Magnetic Field Code - MAFCO (The Modification and Application)

T.F. Yang

October 1972

UWFDM-30

FUSION TECHNOLOGY INSTITUTE

UNIVERSITY OF WISCONSIN

MADISON WISCONSIN

The Preliminary Report on a Three Dimensional Magnetic Field Code - MAFCO (The Modification and Application)

T.F. Yang

Fusion Technology Institute
University of Wisconsin
1500 Engineering Drive
Madison, WI 53706

http://fti.neep.wisc.edu

October 1972

UWFDM-30

THE PRELIMINARY REPORT

ON A THREE DIMENTSIONAL MAGNETIC FIELD CODE - MAFCO

(THE MODIFICATION AND APPLICATION)

by

T. F. Yang

October 1972

FDM 30

University of Wisconsin

These FDM's are preliminary and informal and as such may contain errors not yet eliminated. They are for private circulation only and are not to be further transmitted without consent of the authors and major professor.

Abstract

A magnetic field computor code MAFCO-II[1] obtained from Lawrence Radiation Laboratory Liversmore was converted for use on UNIVAC-1108. The code can calculate the magnetic field, at any point in space, of current carrying filements of arbitrary geometry and also the continuation of the magnetic field line passing through any desired point in space. The code has also been modified to include the circular coil of rectangular cross-section.

Introduction

In the MAFCO code it is assumed that the currents are dc and no permeable material is present. The current elements are taken to be of geometrical size (infinitesmall thin filements). The desired configuration of current-carrying conductors is approximated by a combination of following:

1. circular loops with any designated position and orientation in space specified by the following parameters.

   (x, y, z) = coordinates of the center of the loop.

   A = radius of loop.

   α, β = Euler angles specifying the orientation of loop.

   I = Current passing through the loop. I is a positive number for direction shown in Fig. 1.

2. Circular arcs with any designated position and orientation in space specified by the following parameters.

   (x, y, z) = coordinates of the center of imaginary loop formed by extending the arc.

   A = radius of arc

α, β = Euler angles specifying orientation of arc

ϕ_1 = angle between starting point of arc and x, z, plane (see Fig. 16)

ϕ_2 = angle at which arc ends $\phi_2 > \phi_1$

I = current passing through arc, it's direction is shown in Fig. 1.

3. Helices along the z-axis (in the cylindrical coordinate system) with any designated pitch, starting point, and ending point specified by the following parameters.

A = radius of helix.

D = half the distance between turns in z-direction

ϕ_1 = angle between starting point and xz plane.

ϕ_2 = angle at which helix ends = ϕ (see Fig. 2) at end of helix. $\phi_2 > \phi_1$. (Note that ϕ_2 will be greater than 360° in many cases.)

I = current in helix (plus if directed from 1 to 2)

Z_0 = distance that starting point is displaced from z = 0 plane.

4. Straight line with any designated starting and ending points in space.

5. General elements consisting of a list of points which the code connects by straight lines.

For the designated magnetic field configuration, the code will calculate the magnetic field $\underset{\sim}{B}$ (B_R, B_θ, B_z, $|B|$) at Rectagnular Grids of Points. Given some points (R, Θ, Z) along the line S, it will trace out the line giving B and $\int ds/|B|$ (which is useful in some plasma stability calculations) at designated intervals along the line.

For super-conducting magnet design it is important to know the field inside and on the surface of the conductor. Although the conductor can be approximated by many discrete thin filements, the results were found not accurate unless one uses closely space filements for all the conductors. The typical magnet coil for Tokomak has a cross-section of about 1m x 1m, in order to obtain reasonable accurate results it is conceivable that the use of a large number of filements is required. The code can only handle maximum of 200 loops. If there are 12 magnet coils, each coil can only be approximated by 16 loops which is certainly not enough. The code can be modified to handle large numbers of loops, however, the excessive computation time forbids this possibility.

The code is now modified to include the configuration of circular coil of finite cross-section based on a code MAGMAP[2] originally written for solenoid in cylindrical coordinates. The coordinate transformation method used in MAFCO made it possible to modify this code to place a coil at any designated position in space. Henceforth the magnetic field can be computed for the finite size coils in toroidal geometry. The method used in MAGMAP is introduced in the following.

The magnetic field is computed by integrating the Biot-Savart law:

$$\vec{dH} = \frac{i\, \vec{dl} \times \vec{R}\, d\rho\, dz}{10\, |\vec{R}|^3} \tag{1}$$

where

$\vec{H}$ = field (in gauss),

i = current density (in amp/cm^2),

$\vec{dl}$ = directed length of current carrying element (in cm),

$\vec{R}$ = position vector from $\vec{dl}$ to field point (in cm),

$d\rho\, dz$ = element of area perpendicular to $i\, \vec{dl}$ (in cm^2).

The quantities in Equation (1) are illustrated in Figure 1.

The integration of Equation (1) is limited to coils with cylindrical symmetry. Also, the integration is carried out in cylindrical coordinates (ρ, φ, z) after the field components are found by expanding the vector product in Cartesian components.

$$\vec{dl} = -\rho \sin\varphi\, d\varphi\, \hat{i} + \rho \cos\varphi\, d\varphi\, \hat{j} \tag{2}$$

The field point is specified as (P, Φ, Z), whence

$$\vec{R} = (P\cos\Phi - \rho\cos\varphi)\, \hat{i} + (P\sin\Phi - \rho\sin\varphi)\, \hat{j} + (Z-z)\, \hat{k} \tag{3}$$

Combining Equations (2) and (3) gives

$$\vec{dl} \times \vec{R} = \rho(Z-z)\cos\varphi\, d\varphi\, \hat{i} + \rho(Z-z)\sin\varphi\, d\varphi\, \hat{j} + (\rho^2 - \rho P\cos\Phi\cos\varphi - \rho P\sin\Phi\sin\varphi)\, d\varphi\, \hat{k} \tag{4}$$

From (4) and (1) we obtain the Cartesian components of $d\vec{H}$:

$$dH_x = \frac{i(Z-z)\ \rho\ \cos\varphi\ d\varphi\ d\rho\ dz}{10\ [(P\cos\Phi - \rho\cos\varphi)^2 + (P\sin\Phi - \rho\sin\varphi)^2 + (Z-z)^2]^{3/2}}$$

$$dH_y = \frac{i(Z-z)\ \rho\ \sin\varphi\ d\varphi\ d\rho\ dz}{10\ [(P\cos\Phi - \rho\cos\varphi)^2 + (P\sin\Phi - \rho\sin\varphi)^2 + (Z-z)^2]^{3/2}}$$

$$dH_z = \frac{i(\rho^2 - \rho P\cos\Phi\cos\varphi - \rho P\sin\Phi\sin\varphi)\ d\varphi\ d\rho\ dz}{10\ [(P\cos\Phi - \rho\cos\varphi)^2 + (P\sin\Phi - \rho\sin\varphi)^2 + (Z-z)^2]^{3/2}} \qquad (5)$$

By using the relations: $dH\rho = dH_x\cos\Phi + dH_y\sin\Phi$

$$dH_\varphi = -dH_x\sin\Phi + dH_y\cos\Phi$$

and also $\cos\varphi\cos\Phi + \sin\varphi\sin\Phi = \cos(\varphi-\Phi)$

$$\sin\varphi\cos\Phi - \cos\varphi\sin\Phi = \sin(\varphi-\Phi)$$

we obtain the cylindrical coordinate components of $d\vec{H}$:

$$dH_\rho = \frac{i(Z-z)\ \rho\ \cos(\varphi-\Phi)\ dz\ d\rho\ d\varphi}{10\ [\rho^2 - 2\rho P\cos(\varphi-\Phi) + P^2 + (Z-z)^2]^{3/2}}$$

$$dH_\varphi = \frac{i(Z-z)\ \rho\ \sin(\varphi-\Phi)\ dz\ d\rho\ d\varphi}{10\ [\rho^2 - 2\rho P\cos(\varphi-\Phi) + P^2 + (Z-z)^2]^{3/2}} \qquad (6)$$

$$dH_z = \frac{i[\rho^2 - \rho\ P\cos(\varphi-\Phi)]\ dz\ d\rho\ d\varphi}{10\ [\rho^2 - 2\rho P\cos(\varphi-\Phi) + P^2 + (Z-z)^2]^{3/2}}$$

Now we must specify the range of the integrations. These are:

φ = 0 to 2π

ρ = A(1) to A(2) (in cm)

z = B(1) to B(2) (in cm)

where A(1) is the inner radius of a coil

A(2) is the outer radius of a coil

B(1) is the lower limit of a coil along the z axis

B(2) is the upper limit of a coil along the z axis

and the coil has a rectangular cross-section in the ρ-z plane. By setting $\theta = (\varphi - \Phi)$ it is possible to show that $H_\varphi \equiv 0$ and that H_ρ and H_z are independent of the angle, Φ, i.e.,

$$H_\rho = \frac{i}{5}\int_0^{\pi}\int_{A(1)}^{A(2)}\int_{B(1)}^{B(2)} \frac{(Z-z)\ \rho\ \cos\theta}{[\rho^2 - 2\rho P\ \cos\theta + P^2 + (Z-z)^2]^{3/2}}\ dz\ d\rho\ d\theta$$

$$H_\varphi \equiv 0 \qquad (7)$$

$$H_z = \frac{i}{5}\int_0^{\pi}\int_{A(1)}^{A(2)}\int_{B(1)}^{B(2)} \frac{(\rho^2 - \rho P\ \cos\theta)}{[\rho^2 - 2\rho P\ \cos\theta + P^2 + (Z-z)^2]^{3/2}}\ dz\ d\rho\ d\theta$$

For H_ρ (7) gives with the use of standard integral tables:

$$H_\rho = \frac{i}{5}\int_0^{\pi} \cos\theta\ \{(\rho^2 - 2\rho P\ \cos\theta + P^2 + (Z-z)^2)^{1/2} + (P\ \cos\theta)\cdot$$

$$\ln\left[\rho - P\ \cos\theta + (\rho^2 - 2\rho P\ \cos\theta + P^2 + (Z-z)^2)^{1/2}\right]\Big|_{z=B(1)}^{z=B(2)}\Big|_{\rho=A(1)}^{\rho=A(2)}\Big]d\theta \qquad (8)$$

For H_z (7) gives easily

$$H_z = \frac{i}{5}\int_0^{\pi}\int_{A(1)}^{A(2)} \frac{(\rho^2-\rho P\cos\theta)(z-Z)}{(\rho^2-2\rho P\cos\theta+P^2)(\rho^2-2\rho P\cos\theta+P^2+(Z-z)^2)^{1/2}}\Bigg|_{z=B(1)}^{z=B(2)} d\rho\, d\theta$$

Now we may show with some difficulty that

$$\frac{\rho^2 - \rho P\cos\theta}{(\rho^2 - 2\rho P\cos\theta + P^2)\ A} = \frac{1}{A} + \frac{P\cos\theta\ (\rho - P\cos\theta)}{Z\,|Z-z|\,[A - |Z-z|\,]\,A}$$

$$- \frac{P\cos\theta\ (\rho - P\cos\theta)}{Z\,|Z-z|\,[A + |Z-z|\,]\,A}$$

$$- \frac{P^2\sin^2\theta}{(Z-z)^2} \cdot \frac{\frac{d}{d\rho}\left[\frac{\rho - P\cos\theta}{A}\right]}{\left[\frac{P^2\sin^2\theta}{(Z-z)^2} + \left(\frac{\rho - P\cos\theta}{A}\right)^2\right]}$$

where $A = (\rho^2 - 2\rho P\cos\theta + P^2 + (Z-z)^2)^{1/2}$, whence by use of integral tables

$$H_z = \frac{i}{5}\int_0^{\pi} (z-Z)\ln(\rho - P\cos\theta + A) + \frac{P\cos\theta}{2\,|Z-z|}\ln\left[\frac{A - |Z-z|}{A + |Z-z|}\right]$$

$$- \frac{P\,|\sin\theta|}{|Z-z|}\tan^{-1}\left[\frac{(\rho - P\cos\theta)\,|Z-z|}{P\,|\sin\theta|\,A}\right]\Bigg|_{z=B(1)}^{z=B(2)}\Bigg|_{\rho=A(1)}^{\rho=A(2)} d\theta$$

(9)

If the field point is on the axis, P = 0 and (8) and (9) reduce to

$$H_\rho \equiv 0$$

$$H_z = \frac{i\pi}{5}\{[B(2) - Z] \ln \frac{A(2) + [A(2)^2 + (Z - B(2))^2]^{1/2}}{A(1) + [A(1)^2 + (Z - B(2))^2]^{1/2}}$$

$$-[B(1) - Z] \ln \frac{A(2) + [A(2)^2 + (Z - B(1))^2]^{1/2}}{A(1) + [A(1)^2 + (Z - B(1))^2]^{1/2}} \qquad (10)$$

These results may be summarized as follows:

Case 1. Field point is on axis, there is no radial field component and the axial component HZ = H_z is given by (10) in closed form.

Case 2. Field point is off axis, there are both radial and axial field components, HR = H_ρ and HZ = H_z given by (8) and (9) respectively. In this case the integrals (8) and (9) must be computed by approximation since they cannot be evaluated in analytical form.

The current density, i, entering into equation (8), (9) and (10) is the current density per cm^2 of coil cross-section. This is related to the current I in the coil as follows:

$$i = \frac{I}{[B(2)-B(1)][A(2)-A(1)]}$$

Program Input and Output

In concise form, the UNIVAC-1108 control cards and the input format is given in Table I. The symbols for the five different types of current elements were explained in the introduction. The units are follows: all distances are to be measured in centimeters, all angles in degrees, all currents in amperes. The magnetic field will then be given in gauss.

The increment Δ (delta) determines the distance over which the field line is approximated by a straight line. Smaller Δ's give greater accuracy but are also more time-consuming. The desired size of Δ depends on how rapidly the field line is changing direction. For a positive Δ the field line will start in the positive z-direction from the given point (R, Θ, Z). A negative Δ will cause the field line to start in the magnetive z-direction. The printout spacing integer p causes the values of (R, Θ, Z) and B to be printed out at spacings of $p\Delta$ instead of Δ as occurs if p is omitted.

The number of current-carrying elements of each type which can be used in one problem is as follows:

circular loop or coils	200
circular arcs	200
helices	50
straight lines	300 (max.)
general current elements	100 (max.) or 2400 points (max.)

The maximum number of each type of calculation that can be done for one problem is

Grids of points for fields	100
Field lines	100.

All output information is labeled. First, all the input information is printed out to identify the problem. Then columns are printed for "Fields along a line parallel to z-axis" for Delta-z $\neq 0$ and increments Delta-R (if any):

$$R\ \Theta\ Z\ B_Z\ B_R\ B_\Theta\ |B|.$$

If Delta-Z = 0, columns are printed for "Fields in a radial direction" (if any):

$$Z\ \Theta\ R\ B_Z\ B_R\ B_\Theta\ |B|,$$

and finally "Field lines" (if any):

$$S\ R\ \Theta\ Z\ B_Z\ B_R\ B_\Theta\ |B|\ \int\frac{ds}{|B|}\ .$$

The last column contains a running total of the integral $\int ds/|B|$ so that one can obtain the value of this integral between two points by subtracting the values at those points.

Applications

Some calculations of the field line for magnet and diverter designs are presented in the following as sample cases:

A. Single circular coil

The coil has an inner radius of 0.714 cm, outer radius of 3.215cm and thickness of 2.315cm. Some calculated field lines are shown in Fig. 3.

B. Toroidal magnet for Tokomak

Fig. 5 shows some field lines for the first Tokomak design which has major radius of 18m and minor radius of 3m. The magnet has 16 circular coils, the inner diameter of each coil is 6.25m and its' cross-section is 3m x 3m. For saving computer time only the two coils shown in the fig. and one coil below which is not shown are of finite cross-section, the rest are approximated by single loop. Due to symmetry the field lines in each 22.5° sector are the same.

The second Tokomak design has 12.5m in major radius and 2.5m in minor radius. There are 12 D-shape magnet coils. The computation by approximating each D-shape coil with 16 D-shape loops and each of them consisting of 18 connected straight line elements is under study. The code will be modified to carry out the computation exactly using connected finite size arcs and straight conductors.

C. Diverter for Tokomak

Fig. 6, 7 and 8 show the field lines of a diverter design for the first Tokomak design with 18m major radius. The locations of the hoops and the plasma currents which was approximated by 35 loops and the ratios of currents in the hoops with total plasma current are indicated in Fig. 6. Fig. 6 shows the separatrix. Fig. 7 shows the field lines without plasma. In Fig. 8 two hoop was brought in from 12m to 6m to bend more field lines toward the center of the Tokomak for stability reason.

Fig. 9 shows the separatrix of a diverter design for the second Tokomak design with 12.5m in major radius. The locations of the hoops and plasma are indicated in the figure. Only one loop was used for plasma in this calculation. Fig. 10 shows the corresponding field lines without plasma. There are more field lines curved in the right direction (toward the center of the Tokomak) than those curved in the wrong direction.

References

1. W. A. Perkins and J. C. Brown, Lawrence Radiation Laboratory, Livermore, UCRL-7744-RevII., (1966).

2. A. D. McInturff, Brookhaven National Laboratory, AADD-151, (1969).

TABLE I

UNIVAC-1108 CONTROL CARDS

```
@ASG, TL  18., T, $PLOT
@ASG,T  12., F21115000
@ASG, T  13., F21115000
@ASG, T  4., F21115000
@ASG, MT  MAFCO., T, 07053
@MOVE  MAFCO., 3
@COPY, G  MAFCO., TPE$
```

MAFCO INPUT

First card contains the number of problems, plot control, input unit, output unit,* (integer, right adjusted in columns 4T5).

First card of this section contains in (right adjusted) columns:

1-5 Number of LOOPS.

6-10 Number of ARCS.

11-15 Number of HELICES.

16-20 Number of STRAIGHT LINES.

21-25 Number of GENERAL CURRENT ELEMENT groups.

26-30 Number of grids for calculating fields.

31-35 Number of calculations of field lines.

CIRCULAR LOOP cards (one for each loop in this problem) containing X, Y, Z, A, Alpha, Beta, I; Coil Control Format (7F10.1, I5).

ARC CARDS - (two for each arc in this problem) containing on card one X, Y, Z, A, Alpha, Beta, I; Formal (7F10.1); and on card two Phi1, Phi2; Format (2F10.1).

HELIX cards (one for each helix in this problem) containing A, D (Z-distance of half-turn), ϕ_1, ϕ_2, I, distance from XY plane; Format (6F10.1).

STRAIGHT LINE cards (one for each straight line in this problem) containing X_1, Y_1, Z_1, X_2, Y_2, Z_2, current from 1 to 2; Format (7F10.1).

GENERAL CURRENT ELEMENT cards (one group for each element in this problem) containing on the first card, X, Y, Z of the

first point, current along points, number of points, Format (4F10.1, I5).

On following cards, X, Y, Z of succeeding points; Format (3F10.1).

Range of points determining grid at which fields are to be calculated, containing RMIN, Delta-R, RMAX, Angle, ZMIN, Delta-Z, ZMAX; Format (7F10.1).

Calculation of field line cards (one for each line in this problem) containing R, θ, Z, Δ, total length of line, printout spacing integer (omit if 1); Format (5F10.1, I5).

COIL SIZE cards (one for each loop if coil control = 1) containing A1, A2, B1, B2 (4F10.5).

* If plot control = 1, do not plot field intensities.

Input Unit = 5, Output Unit = 6, Data read in from cards, output on printer. For other number the corresponding tape assignments should be used, the input and output will be on tapes.

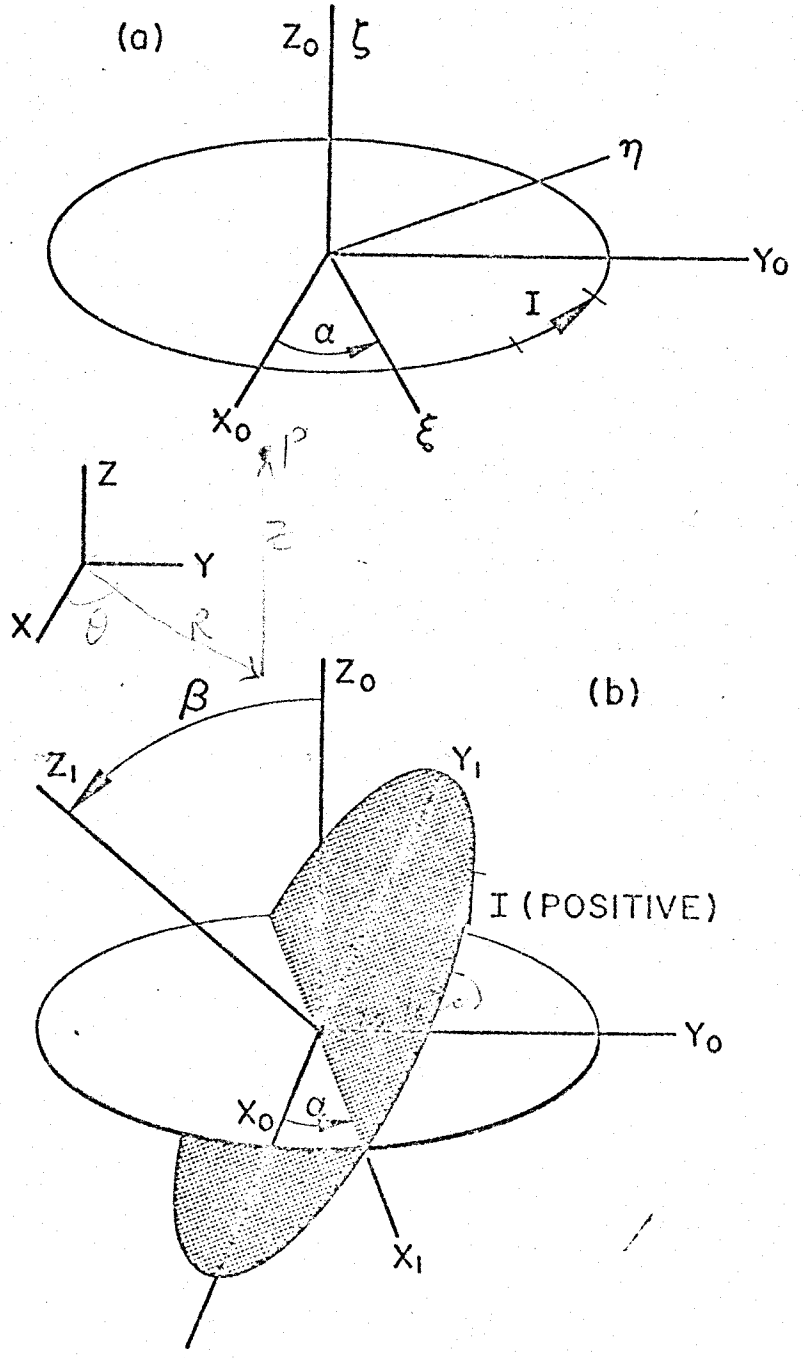

Fig. 1. Position of circular loop in the different coordinate systems. (a) Coordinate system (X_0, Y_0, Z_0) is translated from the (X, Y, Z) (laboratory) system. The (ξ, η, ζ) system is obtained by a rotation through an angle α around the Z -axis. (b) The (X_1, Y_1, Z_1) coordinate system (in which the loop lies in the XY plane with center at the origin) is obtained by a rotation through an angle β around the ξ axis. The arrow shows the direction for positive current.

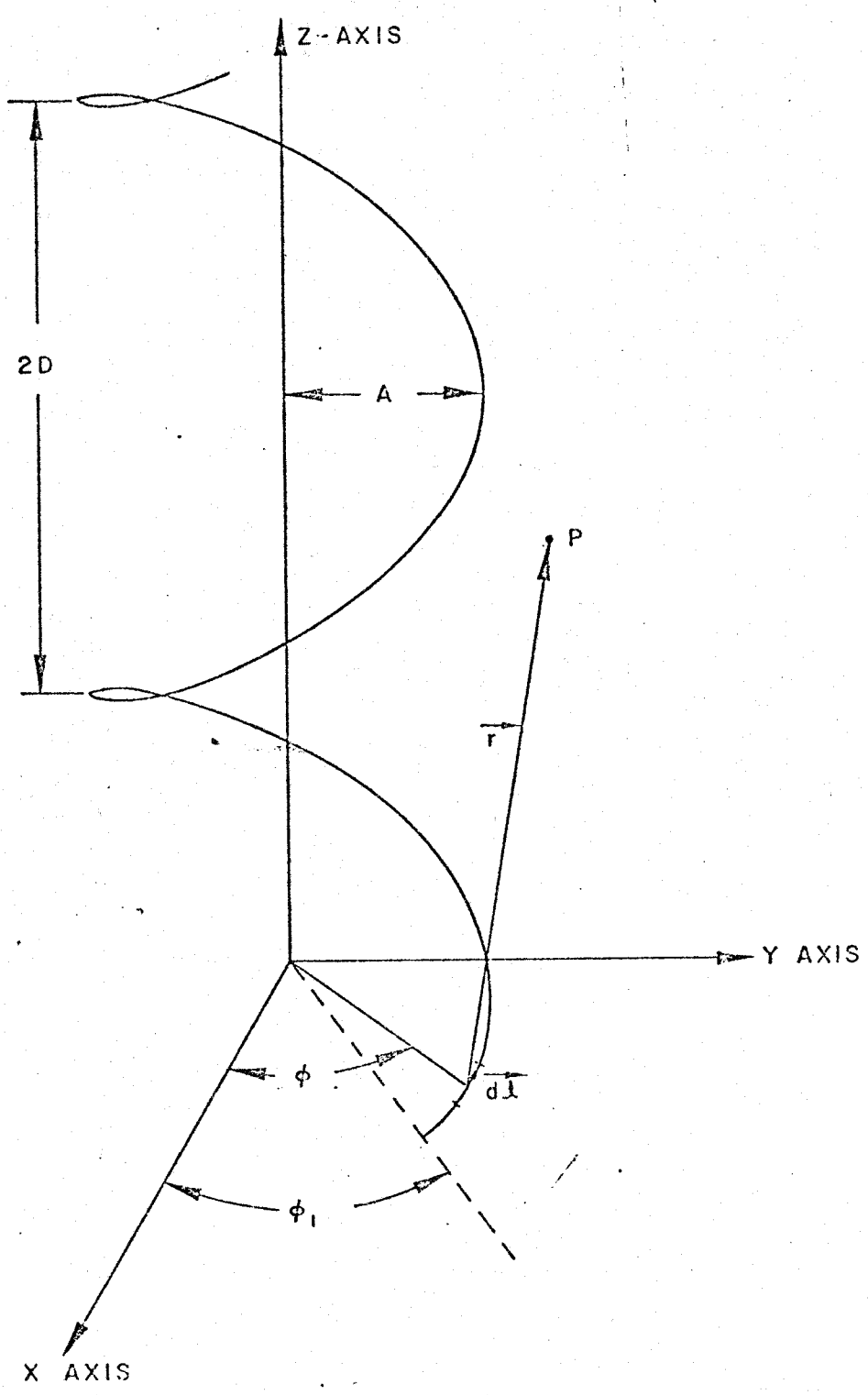

Fig. 2. Helix concentric about the Z-axis in cylindrical coordinate system.

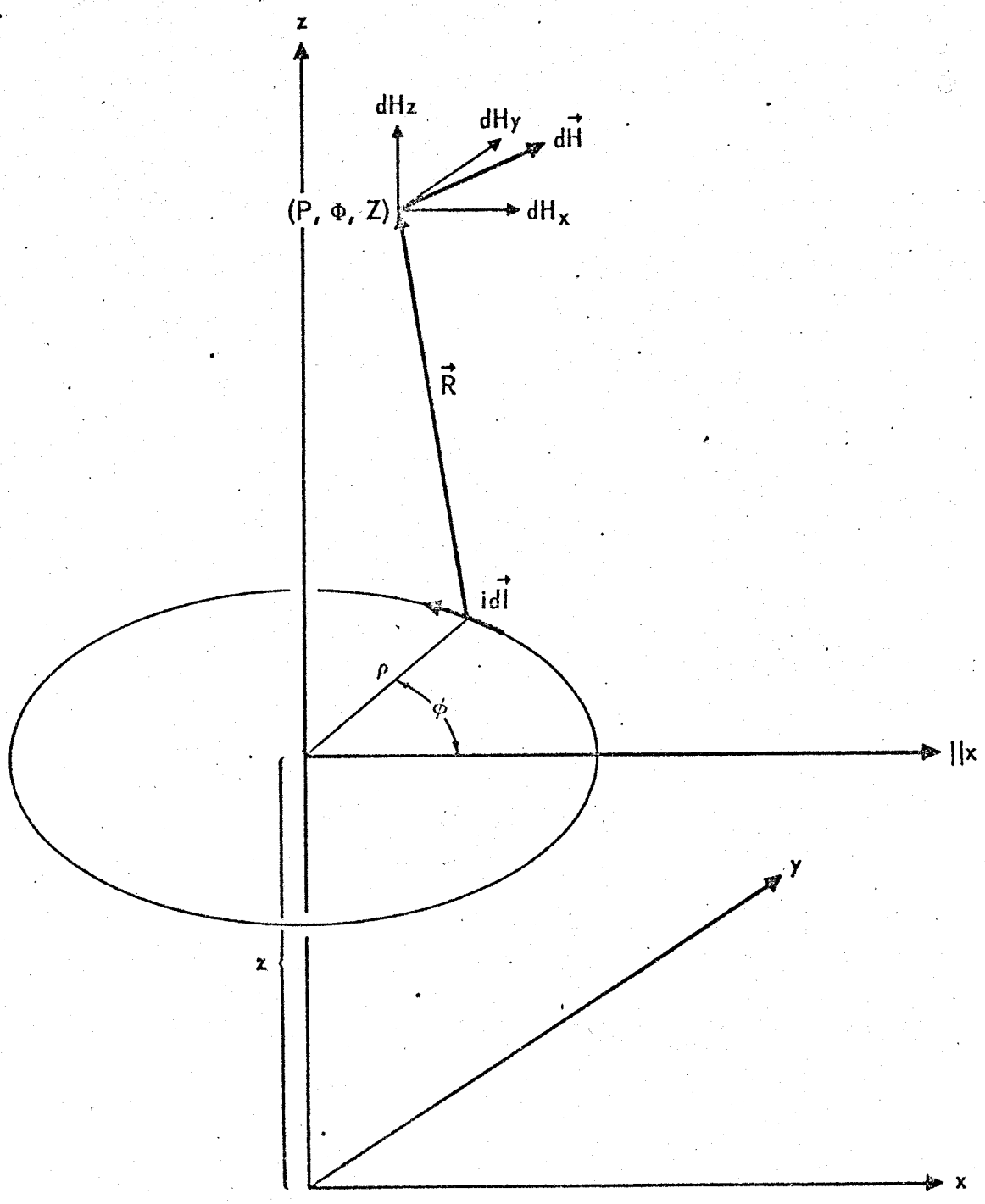

Figure 3 The axis system used to express Equation (1).

TEST CASE (SIGLE COIL)

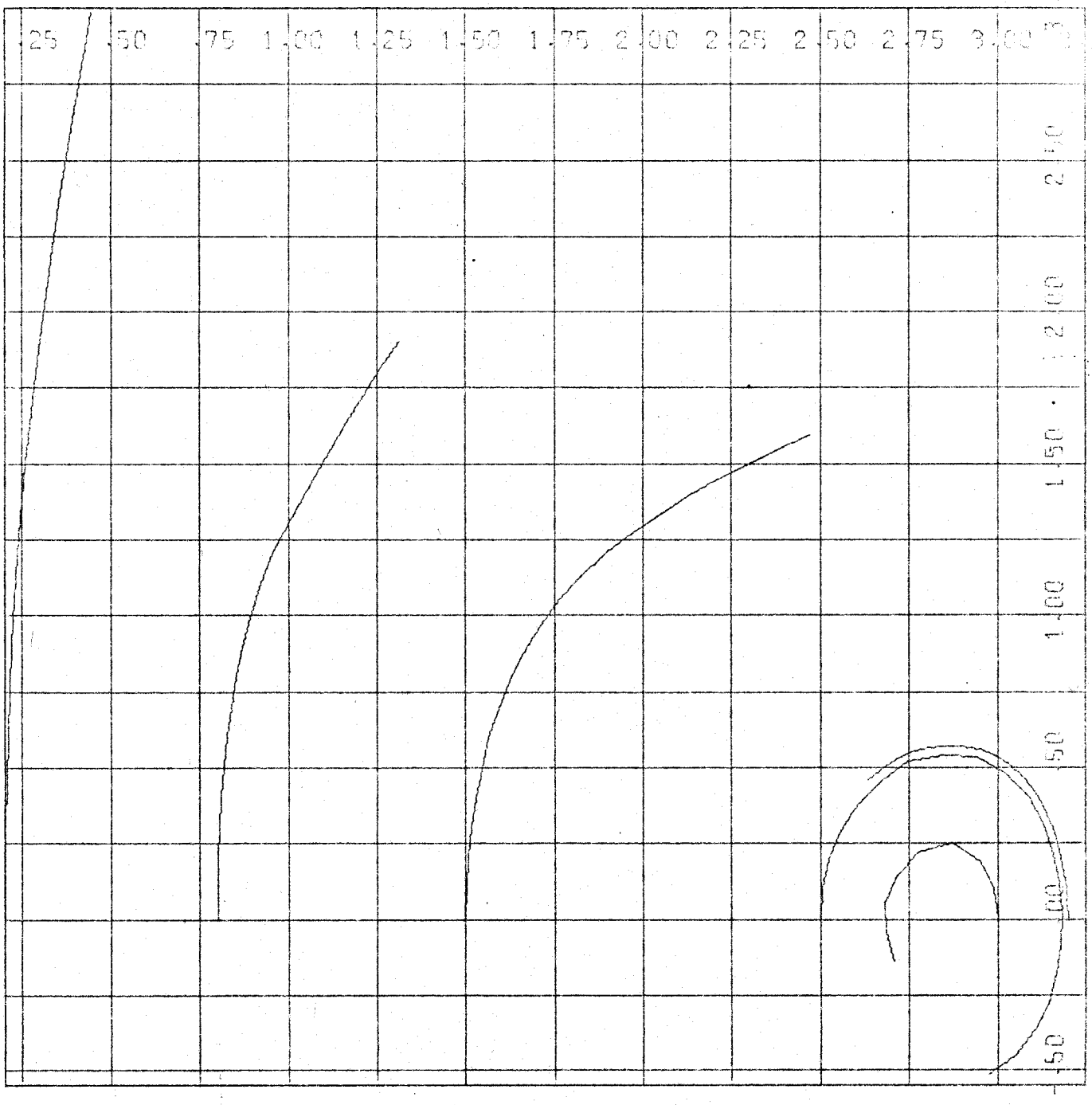

Z - DIRECTION

R - DIRECTION

FIELD LINE PLOT

Fig. 4

Fig. 5

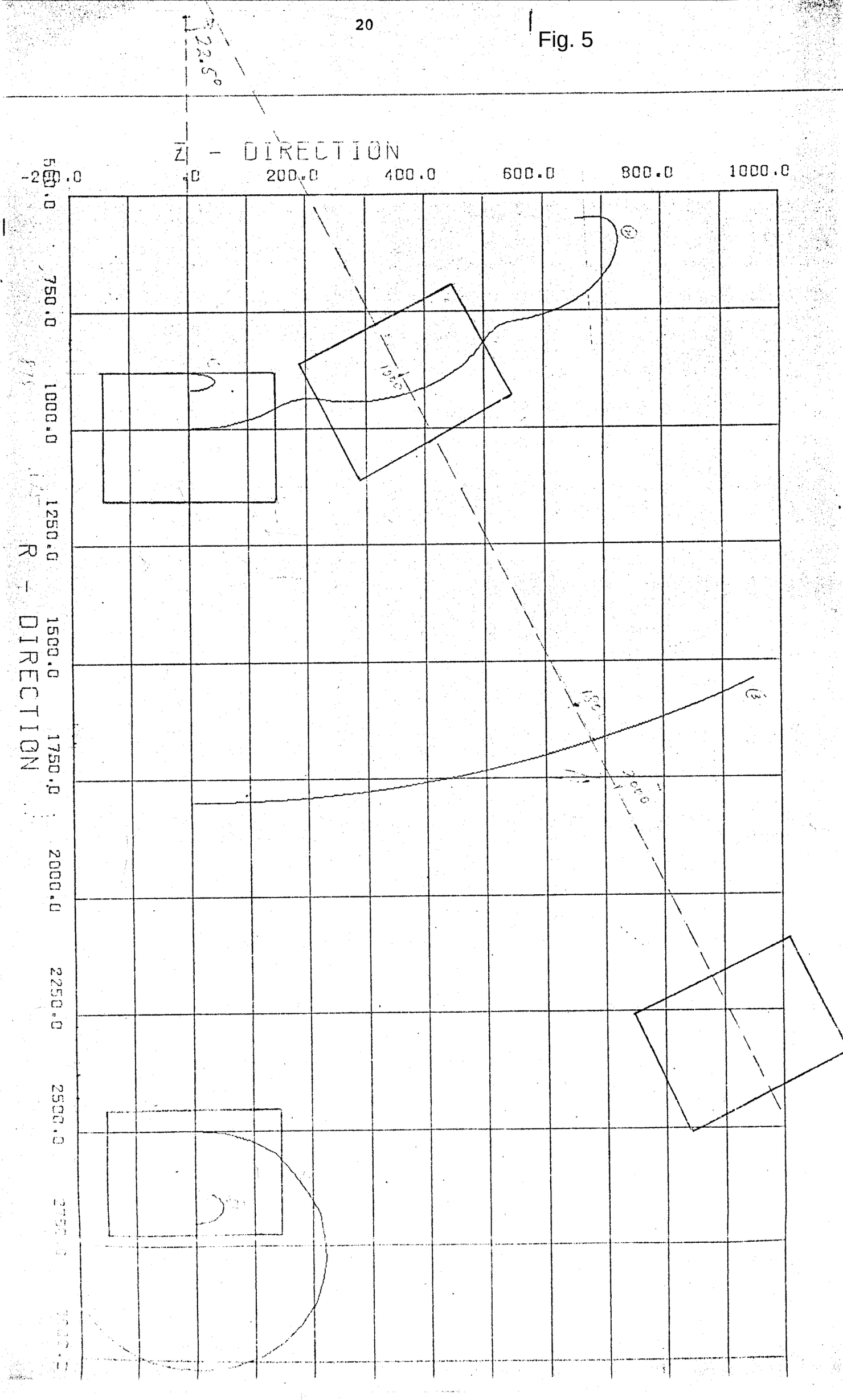
Z - DIRECTION
-200.0
0
200.0
400.0
600.0
800.0
1000.0
R - DIRECTION
500.0
750.0
1000.0
1250.0
1500.0
1750.0
2000.0
2250.0
2500.0
22.5°

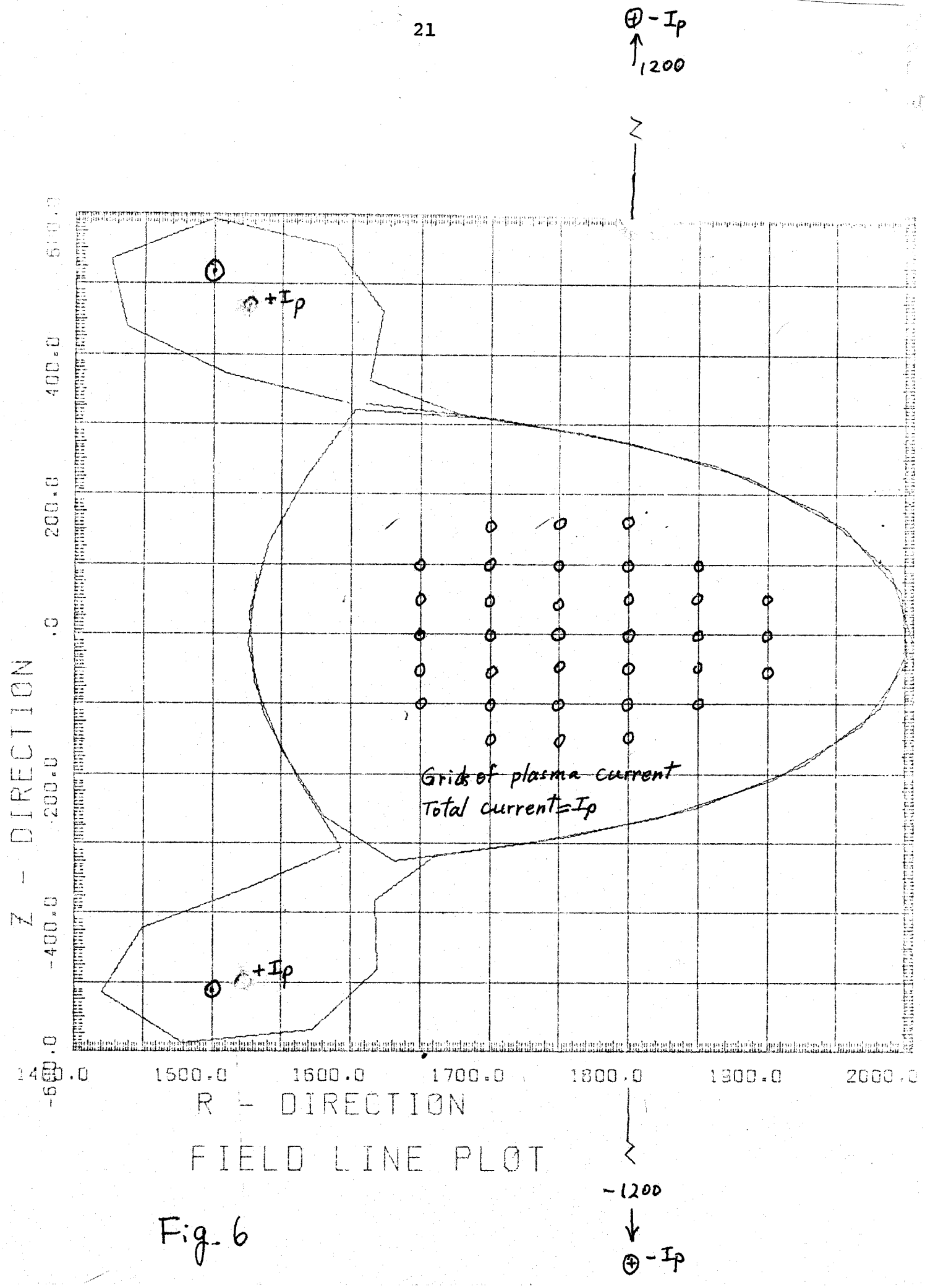
⊕ -Ip
1200
Z
+Ip
+Ip
Grids of plasma current
Total current = Ip
Z - DIRECTION
R - DIRECTION
FIELD LINE PLOT
-1200
⊕ -Ip

Fig. 6

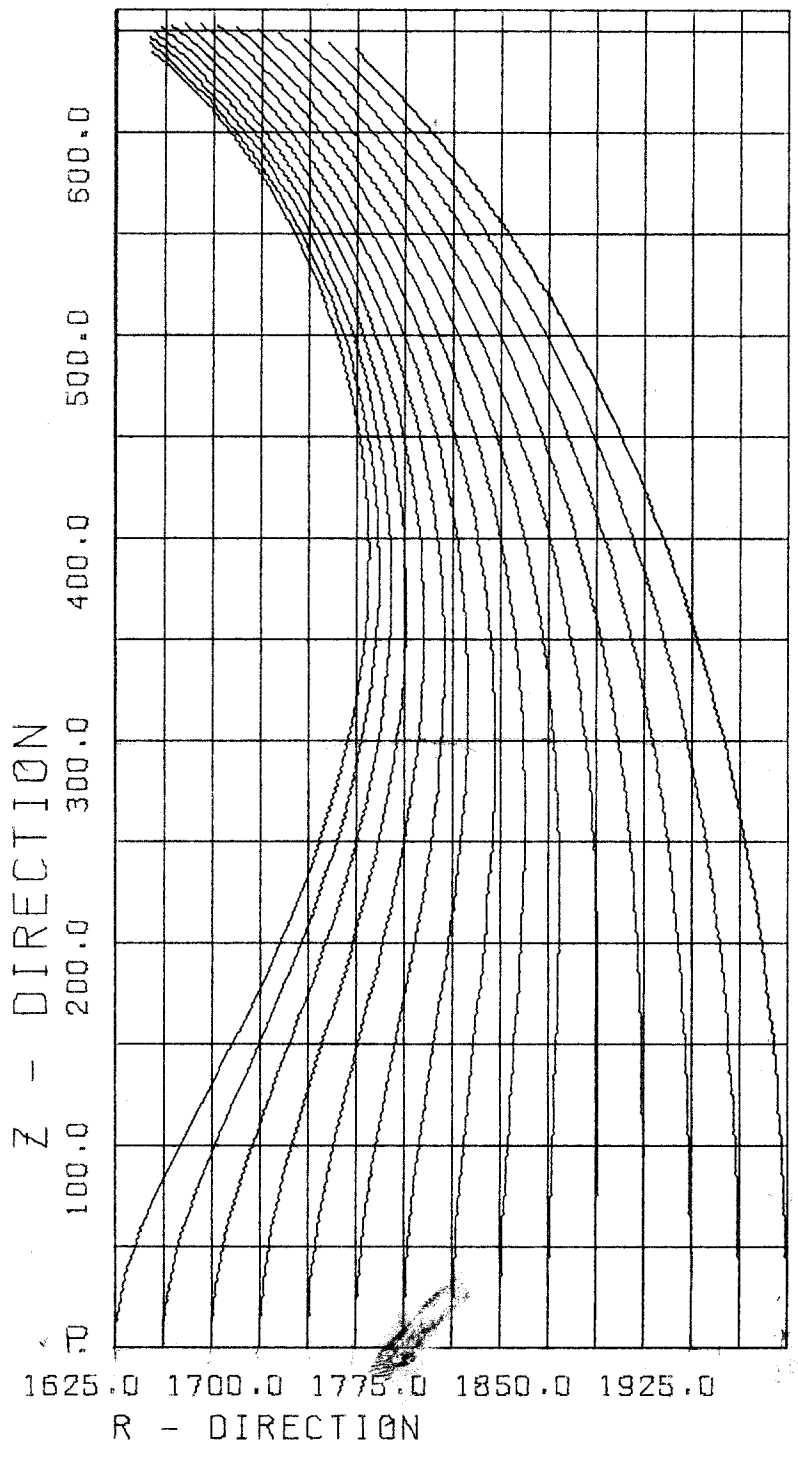

FIELD LINE PLOT (4)

Fig. 7

DIVERTERS IN TOROIDAL COORD.

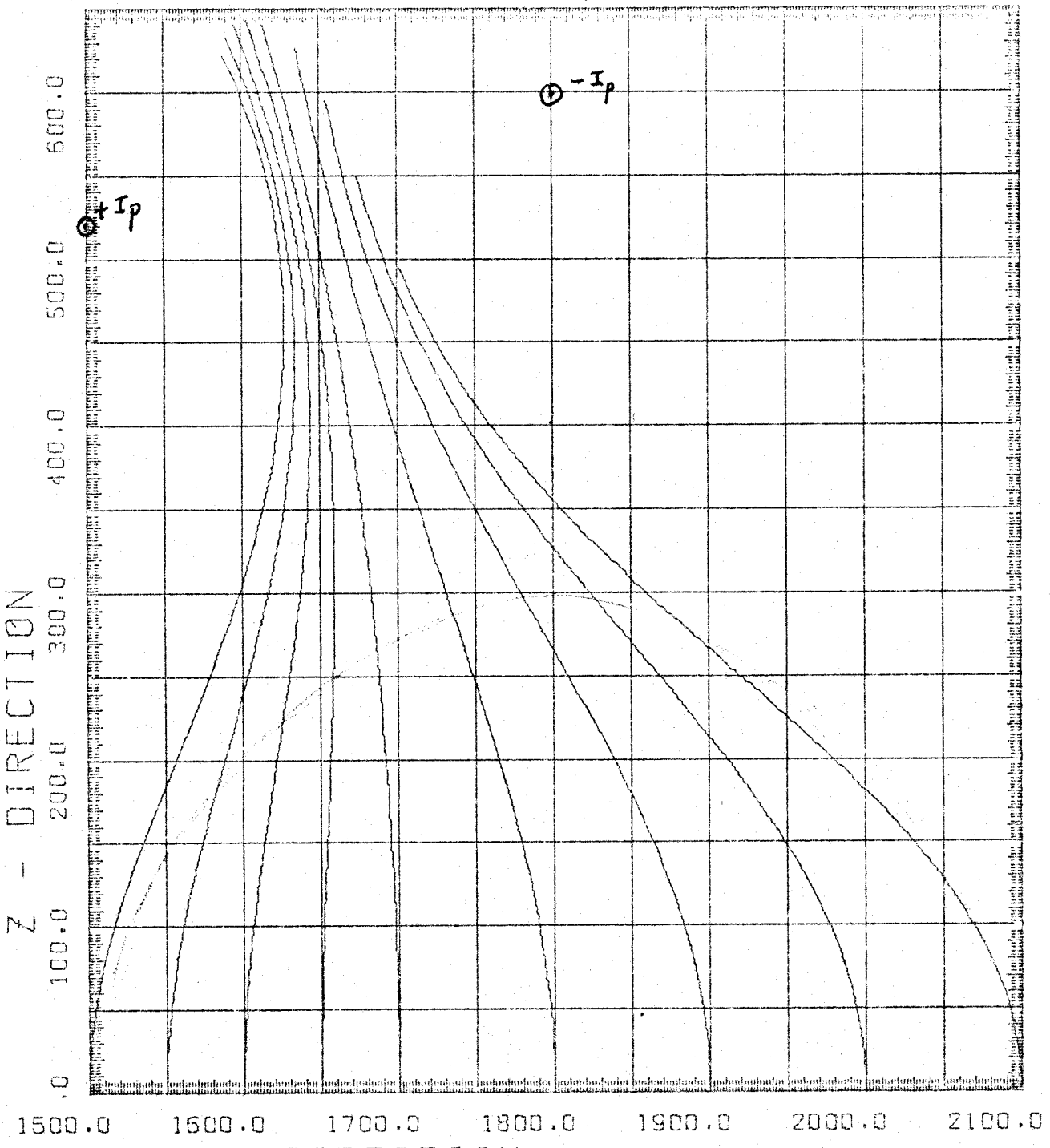

FIELD LINE PLOT

.26 .33 .34 .38 .23 .155 .07

Fig. 8

DIVERTER IN TORUS DESIGN #1C

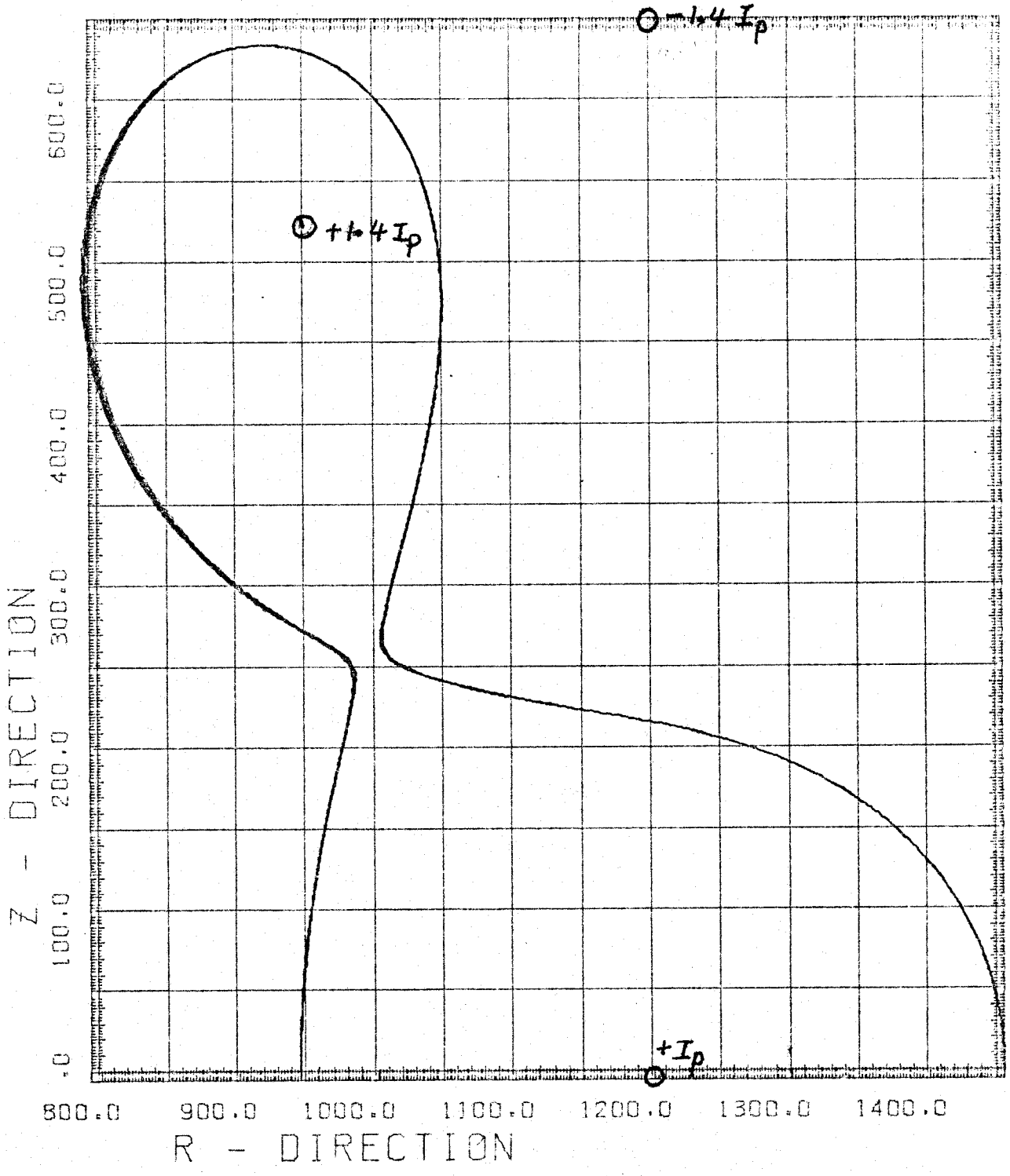

FIELD LINE PLOT

Fig. 9

DIVERTER IN TORUS DESIGN #1E

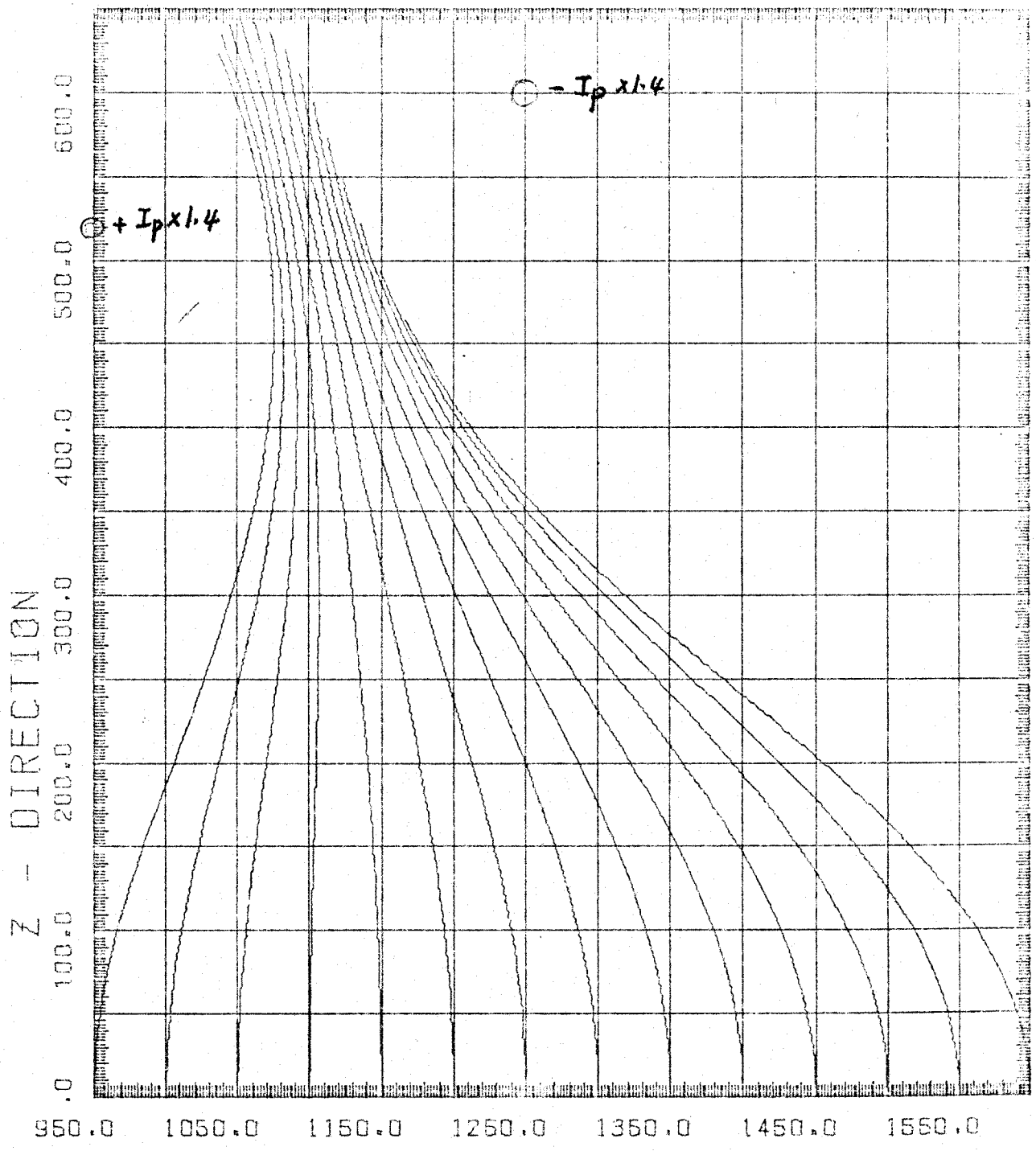

FIELD LINE PLOT

Fig. 10